DOI: 10.1002/cbic.200700386

Fusion Peptides and Transmembrane Domains of Fusion Proteins are Characterized by Different but Specific Structural Properties

Katrin Weise[a, b] and Jennifer Reed*[a]

Membrane fusion is essential for many biological processes. Though there have been many structure and fusion studies of cellular and viral fusion proteins in the last years, their functional mechanism remains elusive. In particular, the structural modes of operation of the transmembrane domains and viral fusion peptides of fusion proteins during membrane fusion have not been elucidated, although work on de novo designed fusogenic peptides suggested that conformational flexibility was necessary. In addition, the use of different and incompatible measurement criteria has made a comparative overview difficult. Here, we report a systematic structural analysis of viral fusion peptides from different fusion protein classes and transmembrane domains of viral and cellular fusion proteins by using circular dichroism spectroscopy. The data that were obtained demonstrate that class I viral fusion peptides show a structural flexibility between helix and irregular secondary structures, whereas fusion peptides of class II viral fusion proteins are characterized by a stable random coil and turn structure. Thus, conformational flexibility does not seem to be a universal criterion for the fusion activity of a fusion peptide. On the contrary, the transmembrane domains of fusion proteins are distinguished by a structural flexibility between helix and sheet structure that is similar to de novo designed unnatural peptides with high fusion activities (M. W. Hofmann et al. PNAS ***2004***, 101, *14776-14781). Thus, the conformational behavior of the fusogenic unnatural peptides most closely resembles that of fusion protein transmembrane domains, and allows them to be used to gain a deeper understanding of the membrane fusion process.*

Introduction

The entry of enveloped viruses into the cell requires the viral membrane to fuse with the target cell membrane. Since membranes do not fuse spontaneously, membrane fusion is mediated by complex protein machinery in living systems. These highly specialized fusion proteins are type I integral membrane proteins and present a large ectodomain, a single transmembrane sequence, a small C-terminal end inside the viral membrane and a specific segment that is involved in membrane fusion that is known as the fusion peptide.[1] Based on their molecular architecture, viral fusion proteins are classified into at least two classes, class I and class II.[1–3] Despite their structural differences, both class I and class II fusion proteins share a number of common features; this suggests that both classes act by a single, universal mechanism to cause membrane fusion.

Fusion peptides (FP) are hydrophobic sequences of the fusion-promoting subunits of fusion proteins that are highly conserved within each family of viruses.[4] They are composed of 20 to 30 mostly apolar amino acid residues, and in general, are enriched in alanines and glycines.[5–7] This unusual amino acid composition suggests that fusion peptides might be conformationally flexible, and might alter their structures depending on the environment.[4] It was proposed that high helicity alone is not sufficient for the fusion activity of the FP. Instead a dynamic equilibrium between helix and non-helix forms of the FP in the membrane environment appears to be essential for the fusion process.[8] Thus, structural flexibility should stand as a criterion for the fusion activity of a fusion peptide.[9,10]

The FP acts in an early stage of fusion, and its insertion into the target membrane leads to a destabilization of the target membrane, and therefore the FP catalyzes the membrane fusion reaction by reducing the activation energy of the process.[5,6,11] In contrast, the role for the transmembrane domain (TMD) of viral fusion proteins lies in the later stages of membrane fusion. It was suggested that the TMD facilitates fusion pore formation and is obligatory for full pore enlargement. These processes require the TMD to span both membrane leaflets to allow membrane destabilization.[12] The greater abundance of glycine residues in fusion protein TMDs produces conformational diversity, which appears to be related to fusion.[13] However, the mechanism by which the TMDs of fusion proteins facilitate pore formation remains unknown.[13]

Structural and functional analyses have revealed remarkable mechanistic similarities between viral and intracellular fusion.[14–16] Both SNARE-mediated fusion and viral fusion appear to be driven by protein folding, releasing enough energy to

[a] *Dr. K. Weise, Prof. Dr. J. Reed*
Department Mechanisms of Biomolecular Interactions
German Cancer Research Center
Im Neuenheimer Feld 280, 69120 Heidelberg (Germany)
Fax: (+49) 6221-423259
E-mail: j.reed@dkfz-heidelberg.de

[b] *Dr. K. Weise*
Present address:
Physical Chemistry I–Biophysical Chemistry, University of Dortmund
Otto-Hahn-Strasse 6, 44227 Dortmund (Germany)

 © 2008 Wiley-VCH Verlag GmbH & Co. KGaA, Weinheim

overcome the energy barrier for the membrane fusion process. Thus, conformational flexibility would need to be a universal property of fusion-promoting protein sequences. A previous work of our group has indicated that the fusion activity of de novo designed unnatural peptides depends on the ratio of α-helix-promoting leucine and β-sheet-promoting valine residues, and is enhanced by secondary-structure-destabilizing proline and glycine residues within their hydrophobic cores. It was shown that for these unnatural peptides, high fusogenicity is correlated with structural flexibility between α-helical and β-sheet structure.[17] To investigate whether the observed conformational flexibility between α-helix and β-sheet is an ubiquitous characteristic of membrane fusion-promoting domains or a special feature of unnatural fusogenic peptides, we carried out a systematic structural analysis of naturally occurring membrane fusion-promoting domains. Therefore, fusion peptides of distinct viral fusion proteins (HA2, HIV-1, RSV, TBEV, and VSV G protein) and transmembrane domains of cellular (Stx 1A and Syb 1) and viral (VSV G protein) fusion proteins were analyzed by circular dichroism spectroscopy according to their secondary structure. Here we report structural properties that are characteristic for the distinct fusion-promoting domains. The results show that viral fusion peptides possess structural properties that are different from those of fusion protein TMDs. In addition, the results demonstrate that the conformational flexibility of the previously analyzed fusogenic unnatural peptides reflects the structural behavior of naturally occurring transmembrane domains of viral and cellular fusion proteins.

Results

To carry out a systematic structural analysis of different membrane fusion-promoting domains, fusion peptides of different viral fusion proteins and transmembrane domains of two SNARE proteins as well as the transmembrane domain of vesicular stomatitis virus G protein were examined with CD spectroscopy. The conformational flexibility of these naturally occurring peptide sequences, that is, their ability to adopt secondary structures depending on the environment, was determined by performing polarity titrations by using aqueous buffer solution and trifluoroethanol (TFE). TFE is known for its structure-stabilizing properties and for enhancing the amount of regular secondary structures in proteins.[18] It also can emulate in some respects the apolar conditions of a membrane environment. To check for oligomerization of the hydrophobic peptides in aqueous buffer solution, concentration dependence studies were carried out (data not shown). To achieve this, CD spectra of the peptides were recorded in Tris–HCl (5 mM, pH 7.5) at concentrations of 10 $\mu g\,mL^{-1}$, 100 $\mu g\,mL^{-1}$ and 500 $\mu g\,mL^{-1}$ in a 1.0 cm, 1.0 mm and 0.2 mm quartz cuvette, respectively. For all fusion-promoting domains, no concentration dependence of the CD spectra could be detected; this indicates that the peptides exist as monomers. In addition, association between peptide molecules can be detected by performing denaturation experiments. Again, no sigmoid curve and thus no association between the analyzed peptide molecules could be detected by heating a solution of 100 $\mu g\,mL^{-1}$ (~38 μM) peptide in glycine–HCl (50 mM, pH 2.6) from 20 °C up to 90 °C (data not shown). In analogy to lysozyme, denaturation experiments were carried out at a low pH in order to bring the melting temperature T_m as far as possible within the temperature range that is available to a water-based system.

Inverse micelles were chosen to reflect the conditions in biological membranes.[19] Because of its optical transparency, the inverse micelle system is much better suited for CD measurements than phospholipid vesicles. The latter show a severe asymmetric scattering in the far-UV region so that to minimize this effect, the use of thinner cuvettes (0.2 mm) and therefore a higher peptide concentration is necessary, which is not appropriate for such hydrophobic peptides. For this reason, secondary structures were studied in a 50 mM AOT/isooctane/water inverse micelle system. The sequences of the analyzed peptides are given in Table 1.

Viral fusion peptides

It is known that human immunodeficiency virus (HIV-1) enters the cell by directly crossing the plasma membrane at neutral pH. In contrast, the influenza virus (HA2 for the membrane-anchoring subunit of haemagglutinin A) is endocytosed after binding to the target cell surface. The low-pH environment of the endosome activates the viral fusion protein, and therefore allows fusion of the enveloped virus with the endosome membrane.[3,20] Because of the two different entry routes of these

Table 1. Sequences of the analyzed peptides[a]

Peptide	Sequence	Classification
influenza virus haemagglutinin A (HA2)	GLFGAIAGFIENGWEGMIDG GCGKKKK	viral class I (N-terminal FP)
human immunodeficiency virus type 1 (HIV-1)	AVGIGAVFLGFLGAAG GCGKKKK	viral class I (N-terminal FP)
rous sarcoma virus (RSV)	RIFASILAPGVAAAQALR GCGKKKK	viral class I (internal FP)
tick-borne encephalitis virus (TBEV)	DRGWGNHCGLFGKG GCGKKKK	viral class II
vesicular stomatitis virus G protein (VSV-FP)	QGTWLNPGFPPQSCGYATVTD GCGKKKK	viral class III
vesicular stomatitis virus G protein (VSV-TMD)	FFFIIGLIIGLFLVL GCGKKKK	viral class III
syntaxin 1A (Stx 1A)	KIMIIICCVILGIVIASTVGGIFA GCGKKKK	cellular
synaptobrevin 1 (Syb 1)	MMIMLGAICAIIVVVIVIYF GCGKKKK	cellular
control peptide L16	LLLLLLLLLLLLLLLL WGCGKKKK	artificial
L16 without GCGKKKK	KKKW LLLLLLLLLLLLLLLL KKK	artificial

[a] all peptides contained free, unmodified termini

 © 2008 Wiley-VCH Verlag GmbH & Co. KGaA, Weinheim

enveloped viruses, the structural analysis of the FP of HA2 was carried out at neutral (pH 7.5) and acidic/fusogenic (pH 5.0) pH, whereas the FP of HIV-1 was analyzed only under neutral conditions. Polarity titrations demonstrated that the fusion peptides of HA2 and HIV-1 exhibit identical structural behavior under fusogenic conditions (Figure 1). Both fusion peptides showed a high content of random coil and turn structure, and a small amount of sheet in a 10 mM Tris–HCl buffer solution (Table 2). While changing the polarity of the environment from polar to apolar, a structural transition mainly from random coil and turn structure to α-helix took place (Figures 1 and 2). In a 90% TFE solution, HA2 FP contained equal amounts of random coil and turn (50%) as well as helix. In comparison to HA2, the structural change was less pronounced for the HIV-1 fusion peptide. The same conformational flexibility between α-helix and random coil/turn structure, but in reverse order, could be observed for both peptides by starting the polarity titrations from TFE and adding buffer with fusogenic pH (data not shown). For the FP of HA2, polarity titrations were also taken at neutral pH. Upon lowering the pH from 7.5 to 5.0, an increase in α-helical structure of 10–20% in the polarity range between 20% and 90% TFE could be detected. Furthermore, the rise in α-helix with decreasing pH occurred at the cost of β-sheet, which appeared as a transient form between 0% and 40% TFE in the polarity titration at neutral pH (data not shown). In inverse micelles, a structural difference existed for both fusion peptides (Figure 3). The FP of HA2 showed a high content of regular secondary structure (74%) with nearly equal amounts of α-helix (38%) and β-sheet (36%), whereas the HIV-1 FP contained a smaller amount of regular secondary structure (28%). In addition, HIV-1 FP consisted of 26% α-helix and only 2% β-sheet under these conditions. However, both fusion peptides have a large amount of α-helix in this inverse micelle system.

As the fusion of the rous sarcoma virus (RSV) envelope with the plasma membrane occurs at neutral pH,[3,20] the structural analysis of the RSV fusion peptide was carried out at pH 7.5. The polarity titration experiment showed a structural flexibility between α-helix and random coil/turn structure for the RSV FP (Figure 1). The fusion peptide of RSV presented a large amount of random coil and turn in buffer solution, and underwent a structural transition to α-helix with an increasing TFE content (Table 2). Simultaneously, the small amount of β-sheet stayed nearly constant over the whole range of polarity. Therefore, the structural behavior of the RSV FP during polarity titrations was comparable to that of HA2 and HIV-1 fusion peptide. The same conformational change could be obtained in reverse by starting the polarity titration with TFE, and by adding buffer solution (data not shown). Measurements in inverse micelles showed a secondary structure for the RSV fusion peptide that consisted of 43% α-helix and 1% β-sheet (Figure 3). These data were also in agreement with the structural properties of the fusion peptides of HA2 and HIV-1 under these conditions, in that they too showed large amounts of α-helical structure.

Like the influenza virus, the tick-borne encephalitis virus (TBEV) enters the cell via the endocytotic pathway, that is, fusion of the endosomal membrane with the viral envelope occurs

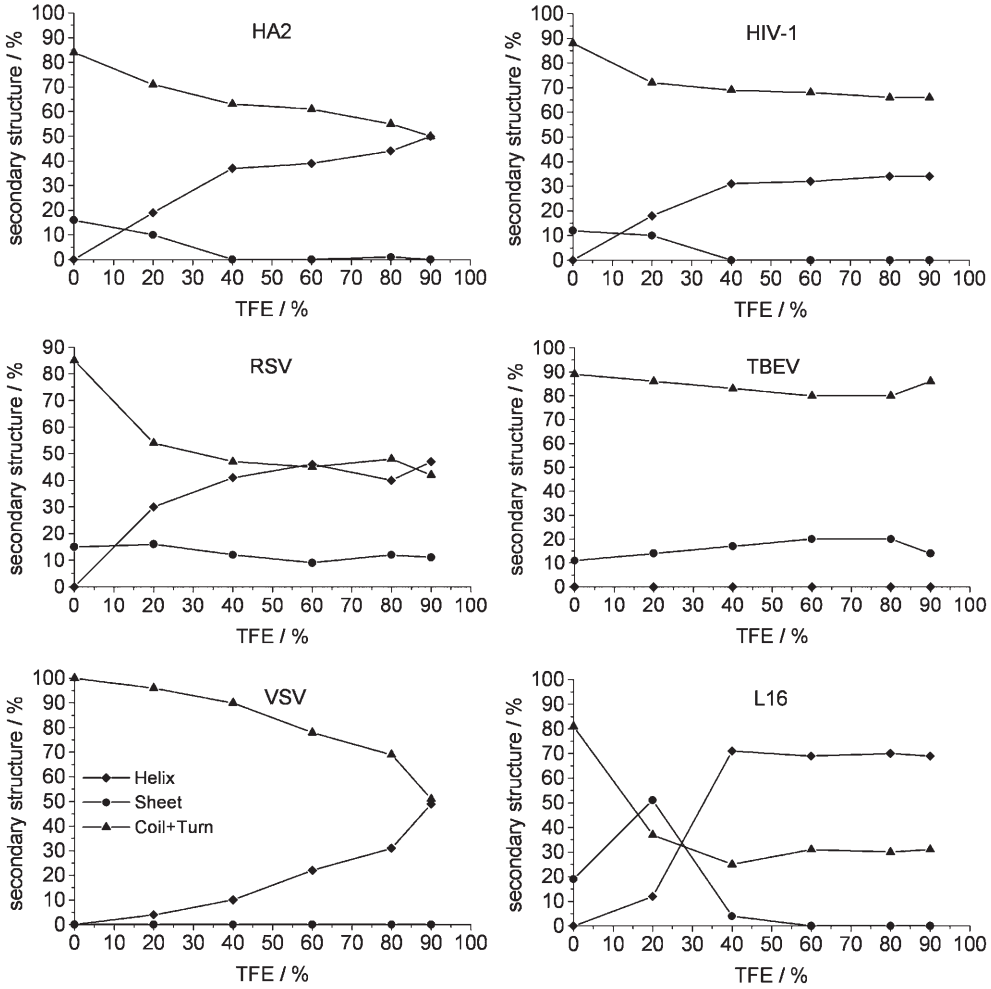

Figure 1. Polarity titrations of viral fusion peptides and L16 as a negative control. Polarity titrations were carried out by starting with 10 mM Tris–HCl buffer solution and adding TFE while maintaining a peptide concentration of 100 μg mL^{-1} (~38 μM). For each fusion peptide, the polarity titration is shown at fusogenic pH, that is, pH 7.5 in the case of HIV-1 and RSV FP, and pH 5.0 in the case of HA2, TBEV and VSV FP. For the negative control L16, the polarity titration is shown at pH 7.5. In the graphic, secondary structures are indicated as follows: ◆: α-helix, ●: β-sheet, and ▲: random coil/turn. Data points represent the means of 2–3 independent measurements.

 © 2008 Wiley-VCH Verlag GmbH & Co. KGaA, Weinheim

Table 2. Data of the polarity titrations for the viral fusion peptides and the negative control peptide L16[a]

	2° structure	TFE content [%]					
		0	20	40	60	80	90
HA2	α-helix	0±0	19±4	37±1	39±1	44±2	50±4
	β-sheet	16±1	10±3	0±0	0±0	1±1	0±0
	coil + turn	84±1	71±1	63±1	61±1	55±1	50±4
HIV-1	α-helix	0±0	18±1	31±1	32±1	34±0	34±0
	β-sheet	12±2	10±1	0±0	0±0	0±0	0±0
	coil + turn	88±2	72±0	69±1	68±1	66±0	66±0
RSV	α-helix	0±0	30±3	41±4	46±1	40±2	47±1
	β-sheet	15±2	16±2	12±4	9±1	12±1	11±1
	coil + turn	85±2	54±1	47±1	45±0	48±3	42±0
TBEV	α-helix	0±0	0±0	0±0	0±0	0±0	0±0
	β-sheet	11±3	14±2	17±4	20±0	20±0	14±1
	coil + turn	89±3	86±2	83±4	80±0	80±0	86±1
VSV-FP	α-helix	0±0	4±1	10±1	22±0	31±1	49±2
	β-sheet	0±0	0±0	0±0	0±0	0±0	0±0
	coil + turn	100±0	96±1	90±1	78±0	69±1	51±2
L16	α-helix	0±0	12±3	71±1	69±1	70±1	69±1
	β-sheet	19±2	51±6	4±1	0±0	0±0	0±0
	coil + turn	81±2	37±8	25±1	31±1	30±1	31±1
L16 without GCGKKKK	α-helix	0±0	25±13	56±4	55±4	57±2	55±6
	β-sheet	18±1	43±5	16±7	12±10	9±10	8±6
	coil + turn	82±1	32±18	28±11	33±13	34±12	37±11

[a] Polarity titrations were carried out by starting with 10 mM Tris–HCl buffer solution and adding TFE while maintaining a peptide concentration of 100 μg mL^{-1} (~38 μM). For each fusion peptide, the polarity titration is shown at fusogenic pH, that is, pH 7.5 in the case of HIV-1 and RSV FP, and pH 5.0 in the case of HA2, TBEV and VSV-FP. For the negative control L16, the polarity titration is shown at pH 7.5.

under acidic conditions.[3,20] Therefore, polarity titrations of the TBEV fusion peptide were carried out at neutral and acidic pH. The experiments showed that the pH did not influence the structural behavior of the TBEV FP during the polarity titration. In addition, the secondary structure of the TBEV FP stayed nearly constant over the whole range of polarity (Figures 1 and 2, Table 2). Identical results could be obtained by carrying out the polarity titration by starting with TFE (data not shown). Nearly the same secondary structure could be detected for the TBEV FP in inverse micelles (Figure 3). Under these conditions the FP of TBEV showed a small content of regular secondary structure (16%) with a much larger amount of β-sheet (14%) than α-helix (2%). Thus, the TBEV FP is characterized by a stable random coil and turn structure.

Vesicular stomatitis virus (VSV) enters the cell by receptor-mediated endocytosis followed by low-pH-induced membrane fusion.[1,20] Hence, polarity titrations were taken under acidic and neutral conditions. By starting the polarity titration from 10 mM Tris–HCl pH 5.0 a conformational transition from random coil and turn to α-helix could be observed with decreasing polarity (Figures 1 and 2, Table 2). Increasing the pH from 5.0 to 7.5 had no effect on the structural behavior of the VSV FP. Again, the conformational transition was reversed when starting the polarity titration from TFE (data not shown). Thus, in titration experiments the VSV FP showed the same structural flexibility as the fusion peptides of HA2, HIV-1 and RSV. In contrast to them, however, experiments in inverse micelles showed a pure random coil and turn structure for the FP of VSV under these conditions (Figure 3).

Compared to the viral fusion peptides, L16, which is an oligoleucine peptide that showed no fusion activity in a standard fluorescence dequenching assay (2.3% liposome fusion after 1 hour) and therefore functions as a negative control (cf. ref. [17]), revealed a completely different structural behavior in polarity titration experiments. There is neither conformational flexibility between α-helical and random coil/turn structure, nor a stable secondary structure as for the TBEV fusion peptide. Instead, a kind of two-phase transition between first random coil/turn structure and mainly β-sheet and second β-sheet and α-helix occurs (Figures 1 and 2, Table 2). A similar structural behavior as for the viral fusion peptides was detected in inverse micelles: the L16 peptide showed 49% α-helix (SD±5%) and 6% β-sheet (SD±6%). This can be explained by the similar secondary structure of the peptides in a solvent of low polarity (as TFE), whereas the structural behavior differs at intermediate solvent polarity.

The host–guest peptide system that was used in this study was introduced by Han and Tamm a few years ago.[21] In this system, the guest peptide (like the FP of the viral fusion protein of HA) is linked via a flexible linker (GCG) to a host peptide (KKKK) that solubilizes the entire peptide. Han and Tamm were able to show that the highly charged host peptide ensured that the peptides remained monomeric in solutions of low ionic strength. In addition, our concentration dependence studies and denaturation experiments (see above) strengthen the case for the monomeric properties of the analyzed peptides. Finally, the linker region that consists of the sequence Gly-Cys-Gly is expected to be conformationally flexible, and thereby allows the uncoupling of secondary structure induction across the host and guest peptide boundary. The host–guest fusion peptides are thought to preserve the native, physiological fusion domain structure, because the host pep-

 © 2008 Wiley-VCH Verlag GmbH & Co. KGaA, Weinheim

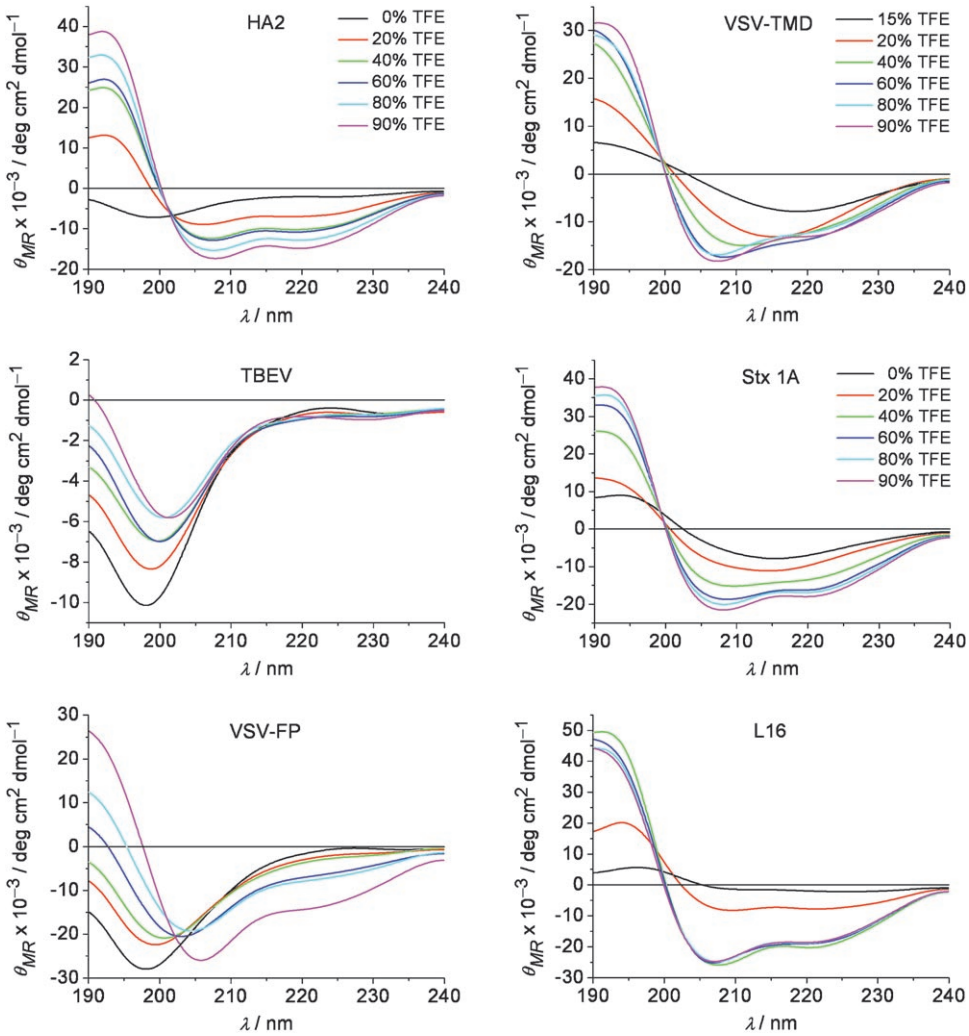

Figure 2. Representative examples of the CD spectra for the polarity titrations by starting from pure buffer solution. For each kind of fusion-promoting domain one example is given: HA2 stands for the structural change from random coil/turn to α-helix (class I fusion peptides), TBEV represents the stable random coil/turn structure of fusion peptides from class II, and VSV-FP shows the structural change from random coil/turn to α-helix of FPs belonging to class III. The viral TMD of VSV G protein as well as the cellular TMD of Stx 1A show a structural change between β-sheet and α-helix which seems to be characteristic for fusion-promoting transmembrane domains. The CD spectra of the control peptide L16 reflect a kind of two-phase transition between first random coil/turn structure and mainly β-sheet and second β-sheet and α-helix. The secondary structure contents of the analyzed CD spectra are given in Table 2 and 3. Color coding of the single CD spectra is identical for all graphs except VSV-TMD, which is given separately in the legend.

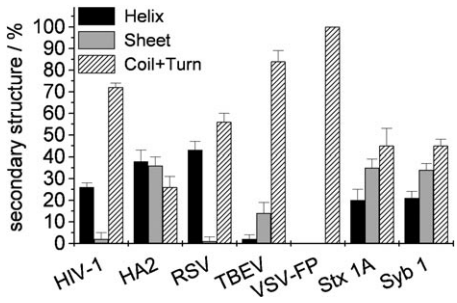

Figure 3. Secondary structures in inverse micelles. The examined fusion peptides and transmembrane domains were measured in an inverse micelle system that consisted of 50 mM AOT/isooctane and 40 μM peptide. The secondary structure content of each fusion-promoting domain is given as follows: black columns: α-helix, light grey columns: β-sheet, and patterned columns: random coil/turn. Data are shown as means ±SD (n = 10–15).

tide replaces, in a sense, the entire polar ectodomain of the viral fusion protein. As the ectodomain and fusion peptide form two separately folded domains at least in HA2, structural influence on the guest peptide by the host peptide should not occur.[4] Nevertheless, we analyzed the same L16 control peptide with a different solubilization system, in which the L16 carries three lysines and one tryptophan at the N terminus, and three lysine residues at the C terminus (Table 1). Lysine residues were used because it was shown that lysine solubilizes the peptide and promotes the monomeric form.[22] The results show the same kind of structural change for the polarity titration experiments as for the L16 that was carrying the sequence GCGKKKK (Table 2). Again, a kind of two-phase transition between first random coil/turn structure and mainly β-sheet and second β-sheet and α-helix occurs. Only a slightly larger amount of α-helix can be detected for the L16-GCGKKKK (up to 15%). In a standard fluorescence dequenching assay the KKKW-L16-KKK showed nearly the same fusion activity as the L16-WGCGKKKK (8.3% and 2.3% liposome fusion after 1 hour, respectively; cf. ref. [17]). Furthermore, nearly the same secondary structure was detected for both peptides in the inverse micelle system (KKKW-L16-KKK 63±8% α-helix, 4±4% β-sheet and L16-WGCGKKKK 49±5% α-helix, 6±6% β-sheet). This comparative analysis was done for two additional peptides, LV16 and LV16G8P9 (cf. ref. [17] and unpublished results), coming to the same conclusion of nearly equal structural properties for both solubilization systems (data not shown). Hence, the host and linker sequence GCGKKKK seems to have no or only a minor effect on the structure of the guest peptide. An analysis of these water-insoluble peptides without a solubilization system would not have been possible.

 © 2008 Wiley-VCH Verlag GmbH & Co. KGaA, Weinheim

TMDs of fusion proteins

The transmembrane domain (TMD) of vesicular stomatitis virus (VSV) G protein was analyzed under neutral and acidic conditions because the virus enters the cell via the endocytotic pathway (cf. VSV FP). Polarity titrations at fusogenic pH 5.0 showed a conformational flexibility of the VSV-TMD between α-helix and β-sheet (Figures 2 and 4). Because of poor peptide solubility in buffer solution at pH 5.0, the polarity titration was started from 15% TFE. Decreasing the polarity of the surroundings by adding TFE led to a structural change from β-sheet to α-helix. Simultaneously, the amount of random coil and turn stayed nearly constant over the whole range of polarity. Consequently, there was a complete transition from one kind of regular secondary structure to the other with a transition point at ~22% TFE (Figure 4 and Table 3). Nearly the same structural behavior was observed for the VSV-TMD by carrying out the reverse polarity titration (data not shown).

Whereas the conformational transition was equivalent for both polarity titrations by starting from TFE and adding buffer with different pH, a remarkable difference was detected for polarity titrations by starting from a buffer solution with a different pH. The VSV-TMD showed only 16% β-sheet but 84% random coil and turn structure in 10 mM Tris–HCl pH 7.5. While adding TFE, a structural change from random coil and turn to α-helix took place between 20% TFE and 40% TFE, which was followed by a change from β-sheet to α-helix in the range of 40% TFE to 60% TFE. The secondary structure content of the VSV-TMD was identical at 90% TFE for both pHs. As the structural transition at pH 5.0 is the one that takes place under fusogenic conditions, conformational flexibility between helix and sheet appears to be crucial for the fusion process.

The same structural flexibility could be observed for the transmembrane domain of the SNARE protein syntaxin 1A (Stx 1A, Figures 2 and 4, Table 3). Changing the polarity from polar to apolar led to a structural transition from β-sheet to α-helix with a transition point at ~33% TFE. The reverse polarity titration gave the same results (data not shown). Intracellular fusion of neurotransmitter-filled presynaptic vesicles occurs at neutral pH. Thus, the TMDs of the SNARE proteins syntaxin 1A and synaptobrevin 1 (Syb 1) were measured only under neutral conditions. In comparison to the TMD of syntaxin 1A, the TMD of synaptobrevin 1 possessed a more restricted conformational

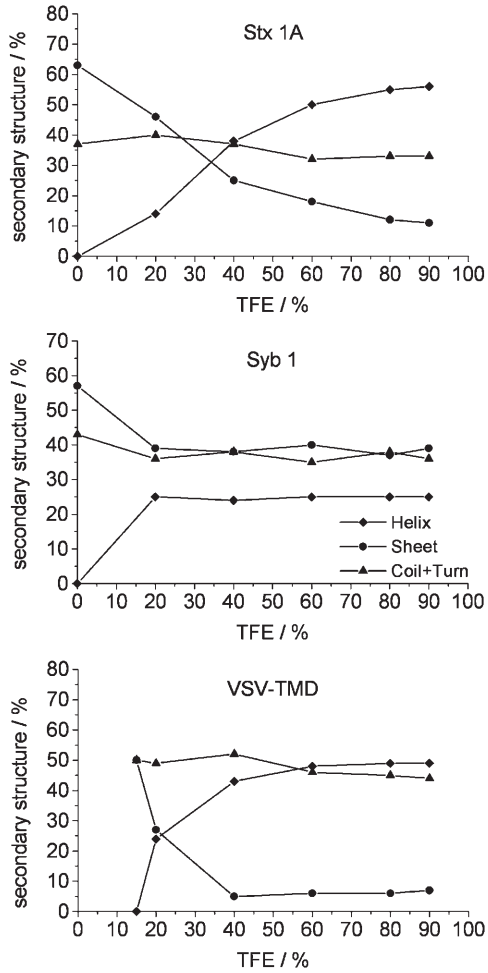

Figure 4. Polarity titrations of the examined transmembrane domains. Polarity titrations were carried out by starting with 10 mM Tris–HCl buffer solution and adding TFE while maintaining a peptide concentration of 100 μg mL^{-1} (~38 μM). For each TMD, the polarity titration is shown at fusogenic pH, that is, pH 7.5 in the case of Stx 1A and Syb 1 TMD, and pH 5.0 in the case of VSV-TMD. In the graphic, secondary structures are indicated as follows: ◆: α-helix, ●: β-sheet, and ▲: random coil/turn. Data points represent the means of 2–3 independent measurements.

Table 3. Data of the polarity titrations for the transmembrane domains[a]

	2° structure	TFE content [%]					
		0	20	40	60	80	90
VSV-TMD	α-helix	0±0	24±1	43±1	48±0	49±2	49±2
	β-sheet	50±5	27±3	5±1	6±1	6±1	7±4
	coil + turn	50±5	49±2	52±2	46±1	45±3	44±1
Syb 1	α-helix	0±0	25±1	24±1	25±1	25±0	25±1
	β-sheet	57±0	39±1	38±2	40±0	37±1	39±1
	coil + turn	43±0	36±1	38±1	35±1	38±1	36±0
Stx 1A	α-helix	0±0	14±1	38±2	50±2	55±2	56±3
	β-sheet	63±1	46±2	25±6	18±2	12±1	11±1
	coil + turn	37±1	40±1	37±4	32±0	33±3	33±2

[a] Polarity titrations were carried out by starting with 10 mM Tris–HCl buffer solution and adding TFE while maintaining a peptide concentration of 100 μg mL^{-1} (~38 μM). For each TMD, the polarity titration is shown at fusogenic pH, that is, pH 7.5 in the case of Stx 1 A and Syb 1 TMD, and pH 5.0 in the case of VSV-TMD.

 © 2008 Wiley-VCH Verlag GmbH & Co. KGaA, Weinheim

flexibility (Figure 4 and Table 3). As the TMD of Stx 1A, the TMD of Syb 1 showed a high amount of β-sheet in buffer solution. However, the addition of TFE resulted in a smaller increase in α-helix such that no transition point could be observed. Nearly the same structural behavior was obtained for the TMD of Syb 1 by carrying out the reverse polarity titration (data not shown). Finally, the secondary structures of the two SNARE protein transmembrane domains were measured in an inverse micelle system (Figure 3). Under these conditions, both TMDs showed a high content of regular secondary structure with nearly equal amounts of α-helix (Syb 1: 21%, Stx 1A: 20%) and β-sheet (Syb 1: 34%, Stx 1A: 35%).

No similarities can be observed between the results for the TMDs and the control peptide, L16. Whereas the structural behavior of the TMDs is characterized by a direct conformational change between α-helix and β-sheet during polarity titrations, the conformational behavior of L16 is distinguished by a kind of two-phase transition (see above). Furthermore, the secondary structure of L16 in inverse micelles differs from that of the TMDs in that it shows a much higher amount of α-helix (49% ±5%) than β-sheet (6% ±6%). Interestingly, the structural behavior of the naturally occurring transmembrane domains of viral and cellular fusion proteins is mimicked by the previously analyzed fusogenic de novo designed unnatural peptides. It was shown that for these unnatural peptides, high fusogenicity is correlated with structural flexibility between α-helical and β-sheet structure.[17] In a length dependency study of the same peptides that contain alternating leucine and valine residues, the highest fusogenicity (58.4%) was detected for a peptide with a hydrophobic core of 16 amino acid residues (LV16), whereas a peptide of 12 residues was too short to span the entire membrane and therefore showed less fusion activity in a standard fluorescence dequenching assay (LV12: 26.6%; M. W. Hofmann and D. Langosch, personal communication). Furthermore, fusion activity decreased again for peptides with longer hydrophobic cores (LV20: 35.5% and LV24: 17.5%), which is due to a loss in the structural flexibility between α-helix and β-sheet (unpublished results). A similar correlation between the length of the hydrophobic peptide core and fusogenicity in vitro was detected by Lorin et al. for peptides that consist of alanine and leucine, which are α-helix-promoting residues.[23] Whereas the peptide of 14 residues that can only traverse one monolayer both exhibits the lowest membrane-binding affinity and shows no significant fusogenicity, peptides of 18 and 22 residues both cross the whole membrane, and show higher membrane-binding affinities as well as fusogenicities. In addition, these hydrophobic TM model peptides were shown to be transmembrane helices in membranes.[23] In contrast to the LV peptides, Lorin et al. did not find an optimum for the length of the hydrophobic peptide core. A critical length requirement of 17 amino acid residues has also been found for the TMD of HA.[24] Hence, the length of the transmembrane domain seems to have a critical function in the later steps of membrane fusion, where the formation and enlargement of the aqueous fusion pore takes place.

Discussion

Structural properties of viral fusion peptides

It has been shown that synthetic fusion peptides are a good model for studying membrane-associated structures and processes that function in viral fusion.[5] Several studies have revealed a direct correlation between the properties of the isolated and intact systems, and thus support the use of small peptides as models for investigating the full protein-mediated fusion process.[5,7,25] However, in previous studies fusion peptides from different viruses were analyzed under varying experimental conditions, which makes a direct comparison of their structural behavior difficult.[25–27] The present CD study allows us to directly compare the conformational properties of different fusion peptides. From the results, it is obvious that the fusion peptides of HA2, HIV-1 and RSV have similar structural behavior, regardless of the placement of the FP in the fusion protein (N-terminal for HIV-1 and HA2 or internal for RSV). The fusion proteins of these viruses are identified as belonging to the viral fusion protein class I.[2,3,28–30] Therefore, fusion peptides of class I viral fusion proteins seem to show a structural flexibility between α-helix and random coil/turn structure under fusogenic conditions. Furthermore, the measurements in inverse micelles point towards an insertion of the fusion peptide into membranes as a helix. The presence of a fairly stable N-terminal (HA2 and HIV-1) or C-terminal (RSV) helix in the fusion peptide sequence appears to be necessary for a tilted insertion of the FP into the membrane, which causes distortion of the bilayer, and therefore catalyzes the membrane fusion process.[30–33] The results for these fusion peptides are in agreement with the experiments of other groups that analyzed the secondary structure of these FPs under related conditions.[21,31–34] The detected structural flexibility can be assigned to the greater abundance of glycine and alanine in the fusion peptide sequence. Mutational analyses have shown that distinct glycine residues (Gly1, Gly4 and Gly8 of HA2 FP; Gly10 and Gly13 of HIV-1 FP) are critical for fusion activity.[35,36]

In contrast to the above-described class I fusion peptides, the FP of tick-borne encephalitis virus is distinguished by a stable random coil and turn structure. The observed structural stability for the TBEV FP region can be explained by a high constraint that is due to multiple interactions. These interactions include several internal hydrogen bonds, one salt bridge (Asp98 and Lys110), and one disulfide bond (Cys74 and Cys105).[37] Consequently, the TBEV FP inserts into membranes as a loop via an aromatic anchor that is formed by Trp101 and Phe108.[38] Since both the fusion peptides of alphaviruses (e.g., semliki forest virus) and flaviviruses (TBEV) are located in a loop that is embedded between two β-strands,[39] it is tempting to speculate that the fusion peptide of semliki forest virus will also interact with the membrane via aromatic residues (i.e., conserved Trp89 and Phe95) and will show a similar stable random coil and turn structure as the TBEV FP. Given that both fusion proteins of flaviviruses and alphaviruses are characteristic representatives of the viral fusion protein class II,[2,3,40]

 © 2008 Wiley-VCH Verlag GmbH & Co. KGaA, Weinheim

fusion peptides of this class seem to be characterized by a stable random coil and turn structure.

The FP of VSV, which possibly belongs to a third class of viral fusion proteins,[1,20] showed structural flexibility between α-helix and random coil/turn structure that is similar to the class I viral fusion peptides. The importance of the conserved Gly124 for fusion activity was demonstrated by mutational analysis.[41] However, a structural difference was detected in inverse micelles that points toward a different interaction with the target membrane. Whereas class I fusion peptides are thought to insert into the target membrane as a helix, the VSV FP did not show α-helical structure in inverse micelles (100% random coil and turn structure). These findings would support the hypothesis that the interaction of the VSV FP with the target membrane occurs mainly at the membrane surface, that is, the fusion peptide does not insert into the membrane.[1] Like VSV, the fusion glycoprotein B (gB) of herpes simplex virus type I (HSV-1) lacks an obvious fusion peptide, but similarity to the fusion peptides of VSV and class II fusion proteins strongly suggests the sequences ^{173}VWFGHRY^{179} and ^{258}RVEAFHRY^{265} act as a fusion peptide.[42,43] In gB, W174, Y179, and A261 seem to be important for fusion, but only F262 is positioned similarly to the aromatic residue in the fusion loop of VSV G protein.[43] The conformation of the fusion loops of HSV-1 appears to be suboptimal for membrane insertion because the hydrophobic residues in the putative fusion loops of gB are surrounded exclusively by charged residues, which has been postulated to prevent insertion. This strengthens the argument for a membrane surface interaction of class III fusion peptides, since HSV-1 and VSV have been proposed to represent this new class of viral fusion proteins.[44]

Structural properties of fusion protein TMDs

The structural properties of viral fusion peptides also differ from those of fusion protein transmembrane domains. Both the TMD of VSV G protein and the TMD of syntaxin 1A showed a conformational flexibility between α-helix and β-sheet under fusogenic conditions. The observed high grade of structural flexibility can be attributed to two main features. First, both TMDs include one (Stx 1A) or two (VSV) glycines that are located in the interior of the TMD. Glycine is known for its helix-destabilizing effect in this position because it forms a flexible hinge and therefore induces a kink into the helix.[45] Second, both TMD sequences present a greater abundance of β-branched amino acid residues. It was speculated that residues with β-branched side chains impart structural flexibility to fusogenic TMD helices.[46] Thus, local deformation or even transient unfolding of these helices might facilitate the restructuring of the lipid bilayer in fusion. Mutational analysis confirmed the importance of such flexibility-promoting residues for the fusion process.[10,45,46]

For several reasons it can be presumed that the TMD of VSV G protein and Stx 1A exist as a transmembrane helix. First, single-pass TMDs such as the VSV G protein and Stx 1A TMD tend to be helical.[47] Second, the appearance of the GxxxG (VSV) or SxxxG (Stx 1A) motif points toward an involvement in high-affinity association of transmembrane helices.[48] Third, these TMDs consist of around twenty mostly hydrophobic amino acid residues, which would just span the hydrophobic part of the bilayer in an α-helical structure.[13] Finally, the observed large amounts of α-helix (20–56%) in membrane-mimetic environments (TFE and inverse micelles) argue for a helical structure of the TMDs in membranes. Since transmembrane domains are known to participate in oligomerization of many different integral membrane proteins, the interactions between α-helical TMDs might contribute to the formation of a prefusion stalk intermediate. Because of the similar structural properties of the VSV-TMD and Stx 1A TMD the results of this work support the hypothesis of a common mechanism for viral and intracellular membrane fusion during the later stages of pore formation, at least.

In comparison, a restricted structural flexibility between α-helix and β-sheet was observed for the transmembrane domain of synaptobrevin 1. The smaller grade of structural flexibility of the Syb 1 TMD can be explained by a lesser abundance of glycine residues in the TMD sequence. Moreover, the location of the single glycine is not as central as in the Stx 1A transmembrane domain, and the SxxxG motif is also missing.

There is evidence, that the pre-transmembrane region of the fusion protein is also involved in viral membrane destabilization during the membrane fusion process. To our knowledge it is not yet clear if and how the pre-transmembrane region is functionally connected to the TMD. However, Langosch et al. were able to show that TMD peptides alone are sufficient to drive fusion of liposomes. In addition, there is proof that the TMDs of cellular and viral fusion proteins fulfill similar structural requirements and might represent autonomous functional domains, which seem to act at a late step in membrane fusion.[10,46] Finally, the arrangement of residues within the conserved amino acid motif in cellular TMD indicated that membrane-spanning and cytoplasmic interaction domains are independent structural units.[10] Furthermore, observations with natural fusion proteins support the results of our study in the sense that structurally flexible TMDs are required for fusion.

Conclusions

By taking together the results for the viral fusion peptides, the present study allows a direct comparison of the structural basis by which fusion peptides from different fusion protein classes' anchor in the target membranes to be made. Thus, given the noticeably different structural behavior of fusion peptides from the different classes that were examined here, the initial steps in the fusion process might be achieved by a variety of mechanisms. Furthermore, structural flexibility seems to be a prerequisite for fusion activity in the case of fusion peptides from fusion proteins of class I and VSV, but not for those fusion peptides that belong to fusion protein class II. As a consequence, conformational flexibility is not a universal property of fusion peptides. In addition, viral fusion peptides show structural behavior that is different to that of previously analyzed unnatural fusogenic peptides.[17]

 © 2008 Wiley-VCH Verlag GmbH & Co. KGaA, Weinheim

In summary, the results for the fusion protein TMDs support the hypothesis of Tamm et al., which states that the TMD of the t-SNARE (in this case Stx 1A) could serve the function of the TMD of the viral fusion protein (VSV G protein), whereas the TMD of the v-SNARE (Syb 1) could serve the role of the viral fusion peptide.[49] However, the structural behavior of the Syb 1 TMD differs from that of viral fusion peptides in that it shows large amounts of β-sheet during polarity titration experiments. In addition, the results demonstrate that the structural behavior of fusion protein transmembrane domains is reflected by the previously analyzed unnatural fusogenic peptides.[17] Consequently, conformational flexibility between α-helix and β-sheet is a phenomenon that takes place not only in de novo designed fusogenic peptides, but is a characteristic feature of naturally occurring transmembrane domains of fusion proteins. This would allow further studies on unnatural fusogenic peptides to get a deeper understanding of the membrane fusion process.

Experimental Section

Peptide sequences: Naturally occurring membrane fusion-promoting domains include fusion peptide sequences of viral fusion proteins and transmembrane domains of viral and cellular fusion proteins. For the present structural analysis, fusion peptide sequences from viruses of different fusion protein classes were used. Class I contains the fusion peptide of influenza virus haemagglutinin A (HA2), GLFGAIAGFIENGWEGMIDG, human immunodeficiency virus type 1 (HIV-1), AVGIGAVFLGFLGAAG, and rous sarcoma virus (RSV), RIFASILAPGVAAAQALR. The fusion peptide of tick-borne encephalitis virus (TBEV), DRGWGNHCGLFGKG, belongs to the viral fusion protein class II. The fusion peptide of vesicular stomatitis virus (VSV-FP), QGTWLNPGFPPQSCGYATVTD, appears to be part of a new class of viral fusion proteins.[1,20] In the second part of the present structural analysis TMDs of two SNARE proteins, syntaxin 1A (Stx 1A) KIMIIICCVILGIVIASTVGGIFA and synaptobrevin 1 (Syb 1) MMIMLGAICAIIVVVIVIYF, as well as the transmembrane domain of vesicular stomatitis virus G protein (VSV-TMD), FFFIIGLIIGLFLVL, were analyzed. The L16 is an oligoleucine peptide of 16 amino acid residues that showed no fusion activity in a standard fluorescence dequenching assay (2.3% liposome fusion after 1 hour) and therefore functioned as a negative control (cf. ref. [17]). For better solubility and handling, a so-called host sequence, amino acids GCGKKKK,[21] was added to all peptide sequences at the C terminus of the fusion peptide and transmembrane domain as well as the negative control peptide L16.

Peptide synthesis and concentration determination: The naturally occurring peptide sequences were synthesized in the peptide synthesis department (Rüdiger Pipkorn) of the German Cancer Research Center in Heidelberg, Germany, by standard solid-phase peptide synthesis (SPPS) technique. The carboxyl group was activated with *O*-(benzotriazol-1-yl)-*N*,*N*,*N*′,*N*′-tetramethyluronium hexafluorophosphate (HBTU) and the free α-amino group was blocked with *N*-(9-fluorenyl)methoxycarbonyl (Fmoc). Peptides were purified by high-performance liquid chromatography (HPLC). In addition, peptide purities were checked by MALDI mass spectrometry and were ≥90% for all samples. Peptide concentrations were determined spectrophotometrically by using tryptophan or tyrosine absorbance at 280 nm or 275 nm and an extinction coefficient of 5600 $M^{-1}cm^{-1}$ or 1400 $M^{-1}cm^{-1}$, respectively. In the case of simultaneous presence of tyrosine and tryptophan, the extinction coefficient was calculated according to Pace et al.[50] The concentrations of peptides that contained only phenylalanine were determined by measuring the absorbance between 250–260 nm and by using an extinction coefficient of 200 $M^{-1}cm^{-1}$. Concentration determinations were carried out on an Ultrospec3000 spectral photometer (Pharmacia; Freiburg, Germany).

Circular dichroism (CD) spectroscopy: CD spectra were obtained by using a Jasco J-710 automatic-recording spectral polarimeter (Jasco, Easton, MD) that was calibrated with β-androsterone (0.05%) in spectral grade dioxane. CD spectra were routinely measured from 190 nm to 240 nm in a 1.0 mm dichroically neutral quartz cuvette at 20 °C by using a time constant of 4 s per scan, a scanning speed of 5.0 nm min^{-1} and a sensitivity of 100 mdeg cm^{-1}. Spectra were the signal-averaged accumulation of four scans with the baseline subtracted. For polarity titration experiments, peptides that were dissolved at 1 mg mL^{-1} in either Tris–HCl buffer (10 mM, pH 7.5 or 5.0) or in 100% trifluoroethanol (TFE) were brought to the respective buffer/TFE ratios while maintaining a peptide concentration of 100 μg mL^{-1} (~38 μM). For measurements in inverse micelles, sodium bis(2-ethylhexyl)sulfosuccinate (AOT)/isooctane/water micelles were prepared by injecting the aqueous peptide solution into a solution of AOT (50 mM) in isooctane and shaking for 2 min. The effective peptide concentrations were 40 μM and spectra were taken immediately after inverse micelle preparation. Signals were averaged eight times, and spectra were measured from 195 to 240 nm. Inverse micelles were prepared with 0.3, 1.0, 1.4, 2.0 and 3.0% aqueous peptide solution. Since the water content had no influence on the peptides' secondary structure (data not shown), the main values were calculated from these five measurements. All CD spectra were converted to mean residue ellipticity (θ_{MR}), and secondary structures were calculated from the CD spectra that were normalized to θ_{MR} by using the program PEPFIT.[51]

Acknowledgements

This work was supported by the Volkswagen Foundation "Conformational Control of Biomolecular Function" Funding Initiative (PW11281).

Keywords: circular dichroism · membrane fusion · peptides · secondary structure · transmembrane domain

[1] A. T. Da Poian, F. A. Carneiro, F. Stauffer, *Braz. J. Med. Biol. Res.* **2005**, *38*, 813–823.
[2] T. S. Jardetzky, R. A. Lamb, *Nature* **2004**, *427*, 307–308.
[3] L. J. Earp, S. E. Delos, H. E. Park, J. M. White, *Curr. Top. Microbiol. Immunol.* **2004**, *285*, 25–66.
[4] L. K. Tamm, X. Han, Y. Li, A. L. Lai, *Biopolymers* **2002**, *66*, 249–260.
[5] J. L. Nieva, A. Agirre, *Biochim. Biophys. Acta Biomembr.* **2003**, *1614*, 104–115.
[6] R. M. Epand, *Biochim. Biophys. Acta Biomembr.* **2003**, *1614*, 116–121.
[7] I. Martin, J. M. Ruysschaert, *Biosci. Rep.* **2000**, *20*, 483–500.
[8] C. W. Wu, S. F. Cheng, W. N. Huang, V. D. Trivedi, B. Veeramuthu, A. B. Kantchev, W. G. Wu, D. K. Chang, *Biochim. Biophys. Acta Biomembr.* **2003**, *1612*, 41–51.
[9] A. Bertocco, F. Formaggio, C. Toniolo, Q. B. Broxterman, R. F. Epand, R. M. Epand, *J. Pept. Res.* **2003**, *62*, 19–26.
[10] D. Langosch, J. M. Crane, B. Brosig, A. Hellwig, L. K. Tamm, J. Reed, *J. Mol. Biol.* **2001**, *311*, 709–721.
[11] S. G. Peisajovich, Y. Shai, *Biochim. Biophys. Acta Biomembr.* **2003**, *1614*, 122–129.

 © 2008 Wiley-VCH Verlag GmbH & Co. KGaA, Weinheim

[12] B. Schroth-Diez, K. Ludwig, B. Baljinnyam, C. Kozerski, Q. Huang, A. Herrmann, *Biosci. Rep.* **2000**, *20*, 571–595.
[13] S. M. Dennison, N. Greenfield, J. Lenard, B. R. Lentz, *Biochemistry* **2002**, *41*, 14925–14934.
[14] T. H. Söllner, *Curr. Opin. Cell Biol.* **2004**, *16*, 429–435.
[15] D. Ungar, F. M. Hughson, *Annu. Rev. Cell Dev. Biol.* **2003**, *19*, 493–517.
[16] J. M. White, J. D. Castle, *Nat. Struct. Mol. Biol.* **2005**, *12*, 382–384.
[17] M. W. Hofmann, K. Weise, J. Ollesch, P. Agrawal, H. Stalz, W. Stelzer, F. Hulsbergen, H. de Groot, K. Gerwert, J. Reed, D. Langosch, *Proc. Natl. Acad. Sci. USA* **2004**, *101*, 14776–14781.
[18] R. Rajan, P. Balaram, *Int. J. Pept. Protein Res.* **1996**, *48*, 328–336.
[19] M. Waks, *Proteins* **1986**, *1*, 4–15.
[20] D. S. Dimitrov, *Nat. Rev. Microbiol.* **2004**, *2*, 109–122.
[21] X. Han, L. K. Tamm, *Proc. Natl. Acad. Sci. USA* **2000**, *97*, 13097–13102.
[22] M. R. de Planque, J. A. Kruijtzer, R. M. Liskamp, D. Marsh, D. V. Greathouse, R. E. Koeppe 2nd, B. de Kruijff, J. A. Killian, *J. Biol. Chem.* **1999**, *274* , 20839–20846.
[23] A. Lorin, B. Charloteaux, Y. Fridmann-Sirkis, A. Thomas, Y. Shai, R. Brasseur, *J. Biol. Chem.* **2007**, *282*, 18388–18396.
[24] R. T. Armstrong, A. S. Kushnir, J. White, *J. Cell Biol.* **2000**, *151*, 425–438.
[25] L. K. Tamm, X. Han, *Biosci. Rep.* **2000**, *20*, 501–518.
[26] E. I. Pécheur, J. Sainte-Marie, A. Bienvenüe, D. Hoekstra, *J. Membr. Biol.* **1999**, *167*, 1–17.
[27] A. Sáez-Cirión, J. L. Nieva, *Biochim. Biophys. Acta Biomembr.* **2002**, *1564*, 57–65.
[28] P. M. Colman, M. C. Lawrence, *Nat. Rev. Mol. Cell Biol.* **2003**, *4*, 309–319.
[29] J. W. Balliet, K. Gendron, P. Bates, *J. Virol.* **2000**, *74*, 3731–3739.
[30] S. F. Cheng, C. W. Wu, E. A. Kantchev, D. K. Chang, *Eur. J. Biochem.* **2004**, *271*, 4725–4736.
[31] X. Han, J. H. Bushweller, D. S. Cafiso, L. K. Tamm, *Nat. Struct. Biol.* **2001**, *8*, 715–720.
[32] L. Vaccaro, K. J. Cross, J. Kleinjung, S. K. Straus, D. J. Thomas, S. A. Wharton, J. J. Skehel, F. Fraternali, *Biophys. J.* **2005**, *88*, 25–36.
[33] S. Kamath, T. C. Wong, *Biophys. J.* **2002**, *83*, 135–143.
[34] D. K. Chang, W. J. Chien, S. F. Cheng, *Eur. J. Biochem.* **1997**, *247*, 896–905.
[35] M. D. Delahunty, I. Rhee, E. O. Freed, J. S. Bonifacino, *Virology* **1996**, *218*, 94–102.
[36] D. A. Steinhauer, S. A. Wharton, J. J. Skehel, D. C. Wiley, *J. Virol.* **1995**, *69*, 6643–6651.
[37] S. L. Allison, J. Schalich, K. Stiasny, C. W. Mandl, F. X. Heinz, *J. Virol.* **2001**, *75*, 4268–4275.
[38] Y. Modis, S. Ogata, D. Clements, S. C. Harrison, *Nature* **2004**, *427*, 313–319.
[39] S. Bressanelli, K. Stiasny, S. L. Allison, E. A. Stura, S. Duquerroy, J. Lescar, F. X. Heinz, F. A. Rey, *EMBO J.* **2004**, *23*, 728–738.
[40] F. X. Heinz, S. L. Allison, *Curr. Opin. Microbiol.* **2001**, *4*, 450–455.
[41] L. Zhang, H. P. Ghosh, *J. Virol.* **1994**, *68*, 2186–2193.
[42] E. E. Heldwein, H. Lou, F. C. Bender, G. H. Cohen, R. J. Eisenberg, S. C. Harrison, *Science* **2006**, *313*, 217–220.
[43] B. P. Hannah, E. E. Heldwein, F. C. Bender, G. H. Cohen, R. J. Eisenberg, *J. Virol.* **2007**, *81*, 4858–4865.
[44] S. Roche, S. Bressanelli, F. A. Rey, Y. Gaudin, *Science* **2006**, *313*, 187–191.
[45] D. Z. Cleverley, J. Lenard, *Proc. Natl. Acad. Sci. USA* **1998**, *95*, 3425–3430.
[46] D. Langosch, B. Brosig, R. Pipkorn, *J. Biol. Chem.* **2001**, *276*, 32016–32021.
[47] L. P. Liu, C. M. Deber, *J. Biol. Chem.* **1998**, *273*, 23645–23648.
[48] W. P. Russ, D. M. Engelman, *J. Mol. Biol.* **2000**, *296*, 911–919.
[49] L. K. Tamm, J. Crane, V. Kiessling, *Curr. Opin. Struct. Biol.* **2003**, *13*, 453–466.
[50] C. N. Pace, F. Vajdos, L. Fee, G. Grimsley, T. Gray, *Protein Sci.* **1995**, *4*, 2411–2423.
[51] J. Reed, T. A. Reed, *Anal. Biochem.* **1997**, *254*, 36–40.

Received: July 13, 2007
Published online on March 10, 2008

 © 2008 Wiley-VCH Verlag GmbH & Co. KGaA, Weinheim